Impact of Water-Assisted Electrochemical Reactions on the OFF-State Degradation of AlGaN/GaN HEMTs

Feng Gao, Swee Ching Tan, Jesús A. del Alamo, *Fellow, IEEE*, Carl V. Thompson, and Tomás Palacios, *Senior Member, IEEE*

***Abstract*— The origin of structural and electrical degradation in AlGaN/GaN high-electron mobility transistors (HEMTs) under OFF-state stress was systematically studied. Hydroxyl groups (OH^-) from the environment and/or adsorbed water on the III-N surface, were found to play an important role in the formation of surface pits during OFF-state electrical stress. The mechanism of this water-related structural degradation is explained by an electrochemical cell formed at the gate edge where gate metal, the III-N surface, and the passivation layer meet. The relationship between structural and electrical degradation in AlGaN/GaN HEMTs under OFF-state stress is discussed. Specifically, the permanent decrease in the drain current is directly linked with the formation of the surface pits, while the permanent increase in the gate current is found to be uncorrelated with the structural degradation.**

***Index Terms*— AlGaN/GaN HEMTs, electrochemical reactions, moisture, reliability.**

I. Introduction

THE last 20 years have seen numerous developments in the design and performance of GaN-based high electron mobility transistors (HEMTs). The unique combination of the high critical electric field of wide band gap materials and the existence of a high mobility 2-D electron gas (2-DEG) allows AlGaN/GaN transistors to be the most promising candidates for high power and high frequency applications [1]. Despite the record-breaking electrical performance achieved by GaN semiconductors, their full market commercialization is still limited by concerns about electrical and structural degradation [2], [3]. Most of the reliability issues in AlGaN/GaN HEMTs are related to the electric field in the AlGaN barrier and/or in the channel region, which can usually exceed 2 MV/cm [1], [3] under high drain bias. The impact of the electric field on the device reliability is especially significant in the OFF-state when the channel is pinched OFF and the electric field is the highest.

The main structural degradation mechanisms studied to date for AlGaN/GaN HEMTs are related to the formation of physical defects (pits and cracks) during high drain OFF-state stress. It has been argued in the past that the field-induced inverse piezoelectric effect of AlGaN material may play a role in causing surface cracking and I_g degradation above a critical voltage [3], [4]. In parallel, it has also been reported that the electrical degradation can occur even below the critical voltage given enough stress time due to a defect percolation process [5]–[8]. Moreover, the pits could also be caused by electrochemical reactions at the surface due to the combination of high electric field and oxygen [9]–[11]. Despite these proposed degradation models, direct experimental evidence of the nature of the structural and electrical degradation in AlGaN/GaN HEMTs are still lacking.

To fully understand the OFF-state degradation in AlGaN/GaN HEMTs, we have carried out investigations of device degradation in a controlled ambient. We have found a relationship between air moisture and surface pitting as demonstrated in Section III. Based on this observation, a water-assisted corrosion-like electrochemical reaction is proposed to explain the mechanism, which is discussed in Section IV. The two necessary conditions for this electrochemical process—the presence of hole carriers and water—are supported by experimental and theoretical evidence in Sections V and VI, respectively. We also find a one-to-one correlation between the drain current degradation and the surface pit formation, while no correlation was found with the gate current degradation. Therefore, we suggest different mechanisms for the two electrical degradation modes in Section VII. The results described in this paper have been reproduced in more than 75 devices across 15 different wafers, both from industry and academia.

II. Device Structure and Experimental Setup

Prototype AlGaN/GaN HEMTs made by an industrial collaborator were used in this paper. Similar results were achieved in transistors fabricated at Massachussetss Institute of Technology (MIT) [10]. The HEMT structure consisted of a 3-nm GaN cap, 14-nm AlGaN barrier, 1 nm AlN interlayer and a thick GaN buffer layer epitaxially

Manuscript received May 6, 2013; revised October 7, 2013 and November 18, 2013; accepted November 22, 2013. Date of publication December 11, 2013; date of current version January 20, 2014. This work was supported by the ONR DRIFT MURI Program. The review of this paper was arranged by Editor B. Kaczer. F. Gao and S. C. Tan have equally contributed to this work.

F. Gao, J. A. del Alamo, and T. Palacios are with the Department of Electrical Engineering and Computer Science, Massachusetts Institute of Technology, Cambridge, MA 02139 USA (e-mail: fenggao@mit.edu; alamo@mit.edu; tpalacios@mit.edu).

S. C. Tan and C. V. Thompson are with the Department of Materials Science and Engineering, Massachusetts Institute of Technology, Cambridge, MA 02139 USA (e-mail: sctan@mit.edu; cthomp@mit.edu).

Color versions of one or more of the figures in this paper are available online at http://ieeexplore.ieee.org.

Digital Object Identifier 10.1109/TED.2013.2293114

0018-9383 © 2013 IEEE. Personal use is permitted, but republication/redistribution requires IEEE permission.
See http://www.ieee.org/publications_standards/publications/rights/index.html for more information.

TABLE I
AlGaN/GaN HEMTs STRESSED IN AMBIENT AIR

	Before Stress	After Stress
I_{dss} (mA/mm)	766	728
I_g (mA/mm)	5.08×10^{-6}	1.40
V_T (V)	-2.98	-3.01
R_d ($\Omega\cdot$mm)	3.74	4.07
AlGaN/GaN HEMTs stressed in vacuum		
	Before Stress	After Stress
I_{dss} (mA/mm)	760	756
I_g (mA/mm)	9.88×10^{-6}	0.924
V_T (V)	-2.99	-2.99
R_d ($\Omega\cdot$mm)	3.76	3.90

I_{dss} and I_g are measured at $V_{gs} = 0$ V and $V_{ds} = 5$ V. The measurements were carried out in ambient air at room temperature and in the dark.

grown on a semi-insulating substrate. An $L_g = 250$-nm T-shaped Pt/Au gate was deposited via metal evaporation. The device surface was passivated by a thick SiN_y layer deposited using plasma enhanced chemical vapor deposition (PECVD).

All the experiments were performed in a atmosphere-controlled probe station with a thermal chuck, humidity sensors, and gas lines, so that specific gases could be introduced into the chamber in a controlled way. These gases can be saturated with water by passing them through a deionized (DI) water bubbler at room temperature so that the humidity increases to close to 100%. The gases can also be dried by flowing them through a drying unit which lowers the humidity to <1%.

III. IMPACT OF MOISTURE ON SURFACE PITTING

The impact of moisture on the structural degradation of AlGaN/GaN HEMTs was studied in the atmosphere-controlled probe station. Two chips from the same wafer with five identical AlGaN/GaN HEMTs on each chip were stressed at high drain OFF-state bias ($V_{gs} = -7$ V and $V_{ds} = 43$ V) for 3000 s (at room temperature in darkness), one in ambient air and the other in a 1×10^{-7} Torr vacuum. The drain and gate current characteristics were first recorded for each fresh transistor and then measured again after electrical stress. To ensure that the after-stress measurements were not influenced by trap-related transients, before the measurements the devices were illuminated for 1 min with ultraviolet (UV) light (254 nm) and kept at rest for 12 h to fully eliminate trapping transients. As summarized in Table I, a small decrease in the drain saturation current I_{dss} and an increase in the drain resistance R_d were observed in HEMTs stressed in ambient air, while the degradation was reduced in HEMTs stressed in a vacuum. The threshold voltage V_T showed no shift after stress in either case.

The gate currents before, during, and after the OFF-state stress were also measured as a function of the stress time. As shown in Table I and Fig. 1, I_g degraded by several orders of magnitude immediately after the application of high voltage stress and did not vary much during continued stressing for devices stressed in both air and vacuum. The during-stress gate currents are also shown in the inset of Fig. 1 and these values will play a role in quantitatively examining

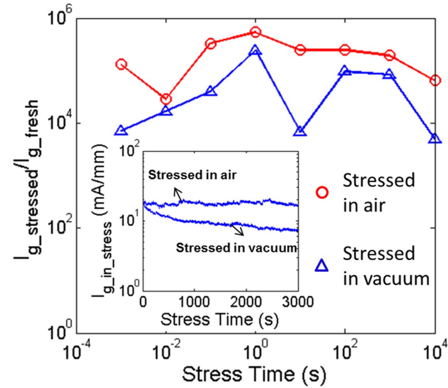

Fig. 1. Ratio of after-stress gate current ($I_{g_in_stressed}$) and unstressed gate current ($I_{g_in_fresh}$) at $V_{gs} = 0$ and $V_{ds} = 5$ V as a function of stress time from 1 ms up to 10 000 s. The AlGaN/GaN HEMTs were stressed at $V_{gs} = -7$ and $V_{ds} = 43$ V in ambient air (red circles) and in a vacuum of 1×10^{-7} torr (blue triangles). The inset shows the during-stress gate current ($I_{g_in_stress}$) for these devices.

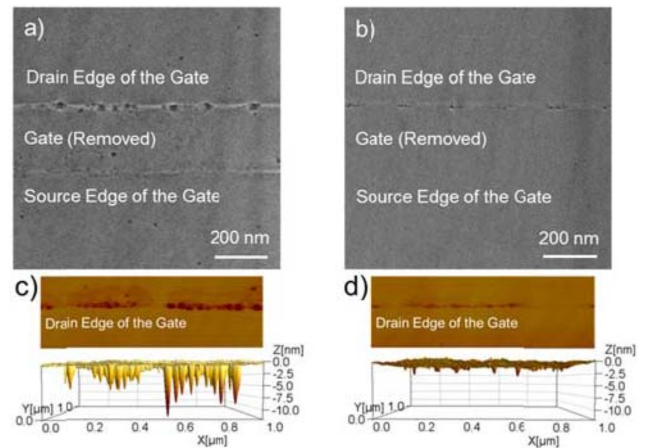

Fig. 2. SEM and AFM analysis of the AlGaN/GaN HEMTs stressed at $V_{gs} = -7$ V and $V_{ds} = 43$ V for 3000 s after gate metals were removed. (a) SEM top view and (c) AFM depth profile in ambient air. (b) SEM top view and (d) AFM depth profile in vacuum of 1×10^{-7} torr.

the mechanisms of the surface pitting, to be discussed in Section V.

The mechanisms behind the above electrical degradation will be further discussed in Section VII.

After electrical stress, the two HEMT chips were subjected to a wet etching process to expose the GaN surface under the gate. The SiN_y passivation was removed by HF etching (HF:H_2O, 1:10) for 2 min; gate metals were removed by aqua regia etching (HCl:HNO_3, 3:1) for 20 min and the samples were subsequently cleaned using a piranha solution (H_2SO_4:H_2O_2, 3:1) for 10 min, rinsed in deionized (DI) water for 1 min and dried using an N_2 gun.

After the removal of the gate metal, the exposed surface in the gate area of these electrically stressed HEMTs was investigated using scanning electron microscopy (SEM) and atomic force microscopy (AFM). Fig. 2 shows the top view and depth profile of the surface area around the gate of the HEMTs that were stressed in ambient air and in vacuum. It can be seen that the mean size and density of the surface pits were significantly higher in the HEMTs stressed in ambient air

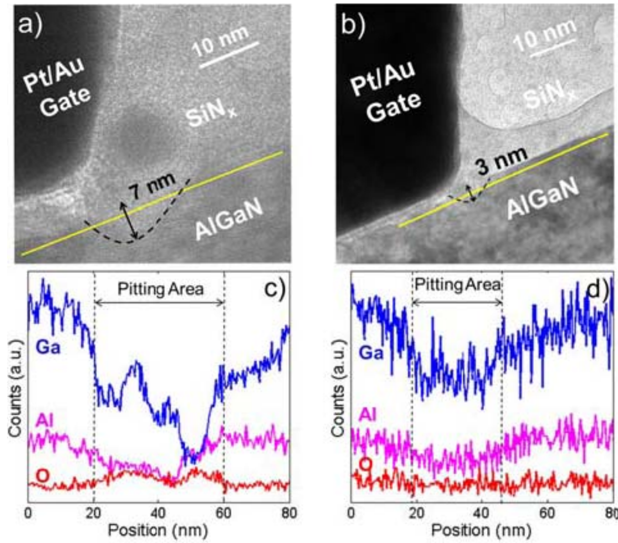

Fig. 3. Cross-sectional TEM images at the drain edge of the gate in the AlGaN/GaN HEMTs stressed at $V_{\mathrm{gs}} = -7$ V and $V_{\mathrm{ds}} = 43$ V for 3000 s in (a) ambient air and in a (c) vacuum of 1×10^{-7} torr. EDX line analysis across the pitting area for the above HEMTs stressed in (b) ambient air and in (d) vacuum. The EDX line scan is indicated as the yellow line in (a) and (b).

than those stressed in vacuum. These results were consistent among the five devices studied in each chip, and reinforce our previous observations on AlGaN/GaN HEMTs fabricated at MIT [9]. It is worth noting that the wet-etching process did not attack the semiconductor, and an unstressed identical HEMT on the same wafer showed a smooth surface around the gate area (not shown), confirming that the surface pitting observed in the AFM analysis was indeed caused by electrical stress.

A different set of two HEMTs (one in each chip) was imaged using cross-sectional transmission electron microscopy (TEM) to study the pits without etching the passivation and gate metals. A smaller pit size was again found in the devices stressed in vacuum when compared with those stressed in ambient air as shown in Fig. 3(a) and (b), respectively. In addition, the material in the surface pits was characterized using energy-dispersive X-ray analysis (EDX). A low concentration of gallium and aluminum and a high concentration of oxygen were observed inside the pit, as shown in Fig. 3(c) and (d), indicating the important role of oxygen in the structural degradation of AlGaN/GaN HEMTs [6], [9], and [11].

Given that surface pitting is reduced when the devices are electrically stressed in vacuum conditions, the oxygen in the pits is most likely from the oxygen gas O_2 and/or moisture H_2O present in ambient air. To discriminate between these two options, another two chips of five identical AlGaN/GaN HEMTs were stressed in the chamber at the same OFF-state bias and duration as above in water-saturated Ar and in dry Ar.

Large I_{dss} and R_d degradation was observed in HEMTs stressed in water-saturated Ar and a significantly lower degradation was observed in HEMTs stressed in dry Ar, while I_g degradations were significant in both cases (Table II). No change of V_T was found. Detailed discussion on the electrical degradation observed can be found in Section VII. In addition, the during-stress gate currents were also recorded

TABLE II

AlGaN/GaN HEMTs STRESSED IN WATER-SATURATED AR

	Before Stress	After Stress
I_{dss} (mA/mm)	794	565
I_g (mA/mm)	3.79×10^{-6}	2.04
V_T (V)	-2.99	-3.00
R_d (Ω·mm)	3.66	5.10
AlGaN/GaN HEMTs stressed in dry Ar		
	Before Stress	After Stress
I_{dss} (mA/mm)	762	759
I_g (mA/mm)	1.12×10^{-5}	0.808
V_T (V)	-2.99	-3.00
R_d (Ω·mm)	3.73	3.90

I_{dss} and I_g are measured at $V_{gs} = 0$ V and $V_{ds} = 5$ V. The measurements were carried out in ambient air at room temperature and in the dark.

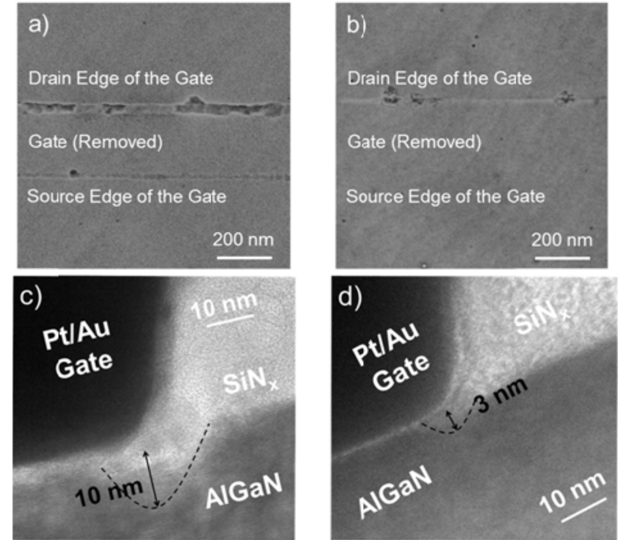

Fig. 4. SEM images of AlGaN/GaN HEMTs stressed at $V_{\mathrm{gs}} = -7$ V and $V_{\mathrm{ds}} = 43$ V for 3000 s in (a) water-saturated Ar and (b) dry Ar, after gate metals and passivations were removed. Cross-sectional TEM images at the drain edge of the gate in AlGaN/GaN HEMTs stressed in (c) water-saturated Ar and (d) dry Ar before etching.

and, as in the air and vacuum experiments, the degradation in I_g happened immediately after the application of the stress conditions, beyond which I_g did not change much during the continued electrical stressing.

After the OFF-state stress, the gate metal and passivation layers were removed as described above, and the exposed surface was subsequently analyzed using SEM. At the same time, several devices in each chip, that were not wet etched, were investigated using cross-sectional TEM. As shown in Fig. 4, the surface pitting was significantly accelerated by water-saturated Ar with respect to dry Ar, which directly supports the water molecules as the cause of the surface pitting.

The difference in the pit sizes between water-saturated and dry Ar was also reproducible in other gas environments, including air, oxygen gas (O_2), nitrogen gas (N_2), and carbon dioxide gas (CO_2). The insignificant surface pitting observed in dry O_2 and dry CO_2 further shows that the oxygen found in the surface pits is indeed from water.

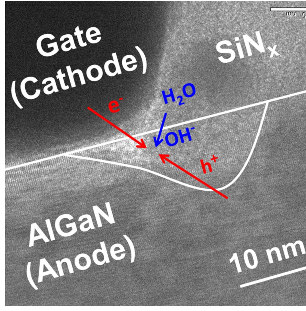

Fig. 5. Electrochemical cell formed at the drain edge of the gate in AlGaN/GaN HEMTs under high OFF-state drain bias (left).

IV. Water-Assisted Electrochemical Reactions

Previous work has found that ambient moisture corrodes GaAs, causing subsequent device degradation [12], [13]. In this paper, we propose that a water-assisted electrochemical reaction or corrosion process is a significant contributor of the surface pitting observed after OFF-state degradation in AlGaN/GaN HEMTs. The gate-SiN_y-$Al_xGa_{1-x}N$ region at the gate edge forms an electrochemical cell which causes anodic oxidation of the $Al_xGa_{1-x}N$ layer (Fig. 5). The reaction starts at the GaN cap surface [11] and then proceeds into the AlGaN barrier during the electrical stress. For simplicity, we use $Al_xGa_{1-x}N$ to indicate both the GaN cap ($x = 0$) and the AlGaN barrier. The proposed reduction–oxidation (redox) reaction between $Al_xGa_{1-x}N$ and water is

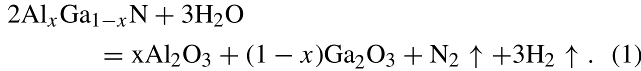

$$2Al_xGa_{1-x}N + 3H_2O = xAl_2O_3 + (1-x)Ga_2O_3 + N_2\uparrow + 3H_2\uparrow. \quad (1)$$

In the electrochemical cell, the gate metal acts as the cathode which provides electrons to the water at the interface between SiN_y and $Al_xGa_{1-x}N$ when the gate-to-drain diode is reversed biased. The corresponding reduction reaction for the water is

$$2H_2O + 2e^- = H_2 + 2OH^-. \quad (2)$$

The electrons contribute to the total gate current. On the other hand, the $Al_xGa_{1-x}N$ layer acts as the anode and is decomposed and subsequently anodically oxidized in the presence of holes and hydroxyl ions (OH^-) following:

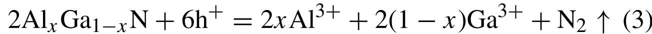

$$2Al_xGa_{1-x}N + 6h^+ = 2xAl^{3+} + 2(1-x)Ga^{3+} + N_2\uparrow \quad (3)$$

and

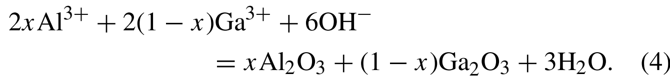

$$2xAl^{3+} + 2(1-x)Ga^{3+} + 6OH^- = xAl_2O_3 + (1-x)Ga_2O_3 + 3H_2O. \quad (4)$$

The decomposition of the $Al_xGa_{1-x}N$ (the GaN cap and the AlGaN barrier) causes the surface pitting that was observed in the SEM, AFM, and TEM analyses. The subsequent formation of the aluminum and gallium oxides explains the origin of the high concentration of oxygen in the pitting area. Moreover, we found a high concentration of gallium in the gate region (more concentrated at the drain edge of the gate) for the AlGaN/GaN HEMTs stressed in both humid and dry environments (including vacuum), while unstressed HEMTs

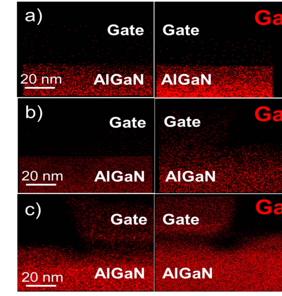

Fig. 6. TEM EDX mapping of gallium (Ga) concentration at the source (left half) and drain (right half) edge of the gate of AlGaN/GaN HEMTs (a) unstressed and (b) stressed at $V_{gs} = -7$ V and $V_{ds} = 43$ V for 3000 s in dry Ar and in (c) water-saturated Ar (right).

showed no gallium in the gate region, as demonstrated in Fig. 6. At the same time, no diffusion of gate metals has been found. This provides good evidence of the $Al_xGa_{1-x}N$ decomposition, as the positive Ga^{3+} ions of (3) would migrate to the negatively biased gate metal along the electric field in the OFF-state. Another interesting feature we find in Fig. 6 is that the Ga atoms actually out-diffuse into the gate metal. Since the room temperature diffusivity of Ga in Au is as large as 7.9×10^{-6} cm^2/s [14] (the corresponding diffusion length $\sqrt{Dt}$ of 1 s is around 28 μm), it is not surprising that this out-diffusion process could occur given an injection source of unbounded Ga^{3+} ions at the gate edge.

In summary, for the proposed corrosion process to happen, it is necessary that:

1) holes are available at the top III-N surface at the gate edge during the high OFF-state drain bias condition;
2) water from the ambient diffuses/permeates through the bulk SiN_y passivation layer and reaches the III-N surface.

The next two sections will discuss these two conditions in detail.

V. Source of Holes

A. Photo-Generated Holes

It is widely accepted that holes are required for the decomposition and oxidation of GaN [15]. A good example is the photo-enhanced chemical (PEC) etching method where UV-generated holes in GaN assist in the formation of Ga_2O_3 in water, after which the oxides are subsequently dissolved in basic solutions [16], [17]. The electrochemical reactions in the GaN PEC-etching process are very similar to the proposed equations (2) and (3). In fact, UV light illumination can significantly accelerate the surface pitting in the OFF-state degradation of AlGaN/GaN HEMTs as well. Fig. 7(a) shows a top-view SEM image (after gate removal) of an AlGaN/GaN HEMT that was stressed at a high drain OFF-state bias ($V_{gs} = -7$ V and $V_{ds} = 43$ V) for 3000 s in ambient air under UV light (254 nm) illumination. In this device, the structural degradation is much more evidence than in devices stressed in darkness [Fig. 2(a)]. TEM images made before removal of the gate metal also showed larger pits in the transistor that was stressed with UV light illumination in Fig. 7(b), than in the one stressed in darkness [Fig. 3(a)].

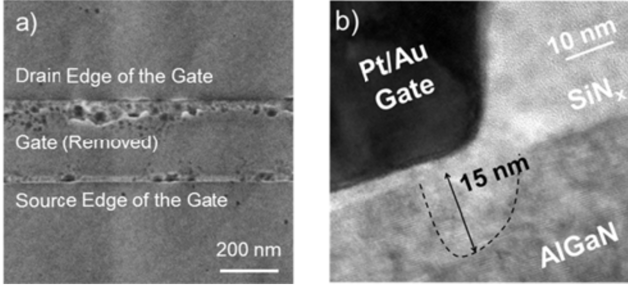

Fig. 7. (a) SEM image of AlGaN/GaN HEMT stressed at $V_{gs} = -7$ V and $V_{ds} = 43$ V for 3000 s with 254-nm UV light illumination in ambient air after the gate metal and passivations were removed. (b) Cross-sectional TEM image at the drain edge of the gate in the same device before etching.

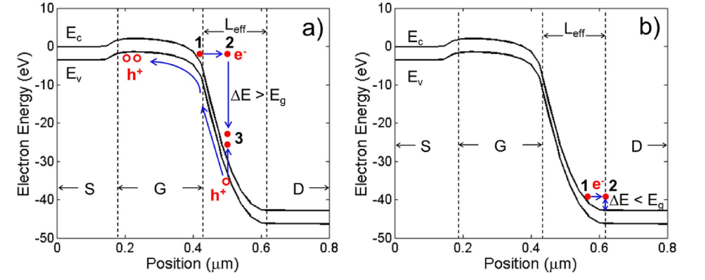

Fig. 8. Schematics of the band diagram in the middle of the 14 nm AlGaN barrier along the lateral direction from source to drain at $V_{gs} = -7$ V and $V_{ds} = 43$ V. Gate electrons enter the high field region at 1 and obtain energy ΔE from the electric field at 2 where impact ionization (a) is triggered when $\Delta E > E_g$ and (b) is not triggered when $\Delta E < E_g$.

The results above show that holes play an important role in the surface pitting phenomenon in OFF-state degradation. However, they do not explain where the holes are coming from when the sample is degraded in the dark. In principle, holes can be generated under high electric field by two mechanisms: 1) impact ionization and 2) interband tunneling. These two different mechanisms are discussed and examined in the following two subsections.

B. Impact Ionization

Due to the large Schottky gate leakage current in most AlGaN/GaN HEMTs and the wide band gap of these materials, the experimental evidence for impact-ionization-induced hole current is controversial [2], [18]–[20]. However, in theory, when gate electrons flow from the gate to the drain in the high electric field region, impact ionization can occur. The electron-initiated hole current density would thus be

$$j_{\text{hole}}^{\text{ion}} = \int \alpha(E) j_g \mathrm{d}x \tag{5}$$

where $j_{\text{hole}}^{\text{ion}}$ is the hole current density caused by impact ionization in the AlGaN barrier or in the channel, j_g is the gate current density and is $\alpha(E)$ the field-dependent impact ionization coefficient, which is exponentially proportional to the negative inverse of the electric field [18]. Therefore, most of the impact ionization occurs in the region with the maximum electric field (E_{max}), so (5) can be written as

$$j_{\text{hole}}^{\text{ion}} \approx \alpha \exp(-\frac{E_i}{E_{\text{max}}}) j_g L_{\text{eff}}, \tag{6}$$

where α is a constant coefficient, E_i is a characteristic electric field for the impact ionization and L_{eff} is the effective length of the high field region. For AlGaN and GaN, E_i is around 34 MV/cm according to [18], [21].

In Fig. 8(a), we schematically illustrate the process. Electrons tunnel from the gate and enter the high field region at 1. They obtain energy ΔE from the electric field at 2 which is larger than the band gap of the AlGaN and thus cause impact ionization at 3. The holes drift toward the source and accumulate under the source side of the gate, which is away from the high field region. Some of these holes can be swept to the negatively biased gate electrode and contribute to the gate current [19]. However, the characteristic bell-shaped gate current curve for impact ionization has never been observed in GaN HEMTs. In addition, hopping conduction dominates the electron leakage current at the gate, which significantly lowers the electron energy further reducing the chances of impact ionization.

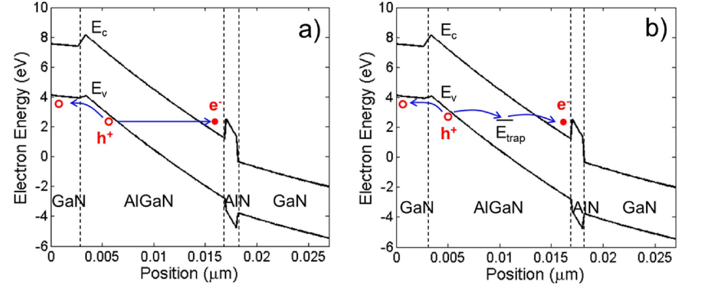

Fig. 9. Schematics of the band diagram at the drain edge of the gate along the vertical direction from the GaN cap to the buffer layer, at $V_{gs} = -7$ V and $V_{ds} = 43$ V. (a) Direct interband tunneling and (b) trap-assisted interband tunneling in the AlGaN barrier.

C. Interband Tunneling

Under a high electric field, electrons from the valence band in the AlGaN barrier could also directly tunnel through the barrier into the conduction band. This process leaves holes in the valence band that can migrate to the surface as illustrated in Fig. 9(a).

This direct interband tunneling would generally obey the Keldysh equation [22]–[24]

$$j_{\text{tunnel}} = \text{CE}^2 \exp\left(-\frac{E_t}{E}\right) \tag{7}$$

where j_{tunnel} is the tunneling current density, C is a constant, E is the electric field, and E_t is a characteristic electric field for direct tunneling in AlGaN and can be explicitly given as [22]

$$E_t = \frac{\pi}{2q\hbar} m_{//}^{1/2} E_g^{3/2} \tag{8}$$

where $m_{//}$ is the reduced effective mass of electrons and holes in the direction of the electric field and E_g is the band gap. Using $m_{//} \approx 0.2\ m_e$ [25], where m_e is the electron mass and $E_g \approx 4.1$ eV for $Al_{0.28}Ga_{0.72}N$ in this paper, we get $E_t \approx 212$ MV/cm, which is around six times larger than the characteristic field for impact ionization. However,

this picture ignores trap-assisted tunneling which has been shown to be responsible for the large Schottky gate leakage current in AlGaN/GaN HEMTs [26]. It is then likely that interband tunneling is also enhanced by defect-related traps in the AlGaN barrier as illustrated in Fig. 9(b), and therefore the characteristic electric field E_t could be significantly lowered in the real devices.

D. Surface Pitting and Holes

In this section, we quantitatively study the nature of the gate leakage current in AlGaN/GaN HEMTs and compare the results with the theoretical estimations of Sections V-B and V-C.

The hole current density in the OFF-state that would be required to explain the structural degradation of AlGaN/GaN HEMTs can be estimated from (3), where the decomposition of one mole of AlGaN corresponds to 3 mol of holes. Therefore, to be able to explain the structural defects observed in GaN HEMTs, the average hole current density over the electrical stressing duration should be

$$\overline{j_h} \propto \frac{3V\rho N_A q}{MAt} = \frac{3\overline{d}\rho N_A q}{Mt} \tag{9}$$

where V is the volume of the surface pits, ρ is the $Al_xGa_{1-x}N$ density, M is the $Al_xGa_{1-x}N$ molar mass, A is the pitting area, t is the electrical stressing duration, M_A is Avogadro's constant and $\bar{d}$ is the average depth of the pits.

For the purpose of providing experimental measurements of the average depth of the surface pits as a function of the electric field, six identical AlGaN/GaN HEMTs on another chip were stressed in ambient air for 1000 s at the same reverse gate bias ($V_{gs} = -7$ V), but at different drain bias from $V_{ds} = 3$ to 53 V with 10 V per step to make the V_{dg} from 10 to 60 V. After stressing and recording of the electrical characteristics, the SiN_y passivation and the gate metal of the samples were wet etched by the procedure described above to expose the surface around the gate. AFM surface analysis was then carried out and the average depth of the surface pits in each transistor was calculated by the scanning probe image processor (SPIP) software in a 1 × 0.1 μm region at the drain edge of the gate. The electric field near the gate was simulated using the 2-D device simulator Silvaco Atlas. As expected, Fig. 10(a) shows that the maximum in the electric field coincides with the triple-line at the gate edge where damage occurs, under all the calculated bias conditions. The maximum electric field is plotted with the average measured pit depth as a function of the drain-to-gate bias in Fig. 10(b).

$\log(\overline{j_h}/E_{\max}^2)$ as a function of $1/E_{\max}$ using the simulated values of $E_{\max}$ and $\overline{j_h}$ calculated from (9) is shown in Fig. 11. It can be seen that $\log(\overline{j_h}/E_{\max}^2)$ follows a linear trend with $1/E_{\max}$ in agreement with (7), supporting the hypothesis that hole generation is caused by interband tunneling. The slope of the fitted line corresponds to the characteristic tunneling field in the AlGaN barrier which is around 7.7 MV/cm. This value of E_t is much smaller than 212 MV/cm, probably due to the existence of trap-assisted interband tunneling [Fig. 9(b)].

At the same time, $\log(\overline{j_h}/\overline{j_g})$ as a function of $1/E_{\max}$ is also plotted in Fig. 11 using the in-stress gate current

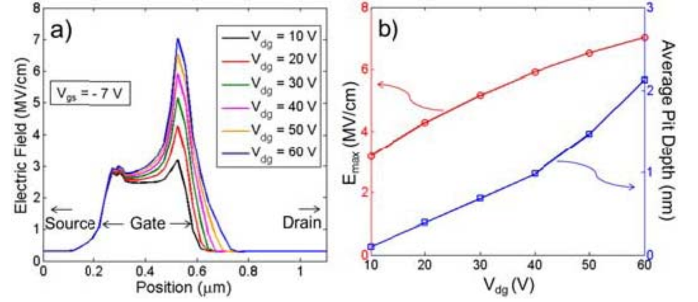

Fig. 10. (a) Simulated total electric field as a function of lateral position in the AlGaN barrier. The values are averaged over the thickness of the AlGaN barrier in the vertical direction. (b) Extracted maximum electric field at the drain edge of the gate and average pit depth measured as a function of the drain-to-gate bias.

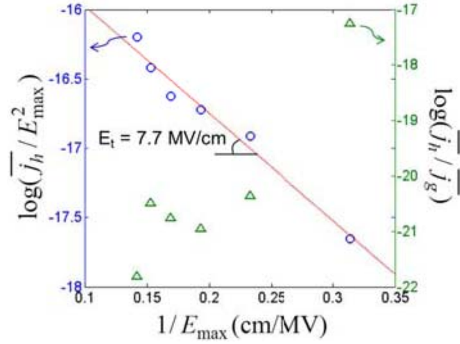

Fig. 11. $\log(\overline{j_h}/E_{\max}^2)$ (blue circles) and $\log(\overline{j_h}/\overline{j_g})$ (green triangles) as a function of $1/E_{\max}$. The number of holes extracted from the volume of the pits seems to follow the interband tunneling model (left y-axis) and not the impact ionization model (right y-axis).

averaged over the stress time $\overline{j_g}$ (as indicated in Fig. 1) on a 50 × 0.25 μm^2 gate area measured during the OFF-state electrical stressing for each transistor. As can be seen, the hole current needed to feed the growth of the pits is just a very small component of the total gate current. More importantly, $\log(\overline{j_h}/\overline{j_g})$is an increasing function of, $1/E_{\max}$ which opposes (6) and indicates that the holes that contribute to pitting are not the result of impact ionization.

Given the experimental evidence above, the holes needed for the electrochemical reactions discussed in Section IV are likely to arise through trap-assisted interband tunneling in the AlGaN barrier. However, to fully understand the mechanisms of the impact ionization and interband tunneling in AlGaN/GaN HEMTs, further work on modeling and direct hole current measurements are needed.

VI. Source of Water

In addition to holes, the proposed electrochemical reaction requires a source of water. In ambient air, there exists a thin layer of adsorbed water on the surface of most solids [27]. Moreover, ambient water can diffuse or permeate through bulk solids with a rate defined as the water vapor transmission rate (WVTR). For a thick (>100 nm) PECVD SiN_y passivation layer, this rate is in the order of 0.01–0.1 g/m^2/day [28], [29]. In fact, the WVTR is an important limiting factor on the total electrochemical reaction described in (1) and can be

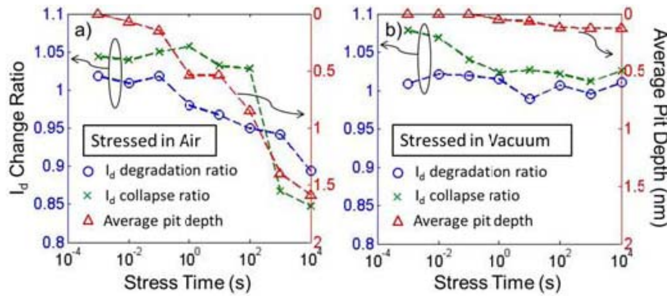

Fig. 12. Drain current (I_d) degradation ratio (blue circles) defined as the after-stress I_d divided by unstressed I_d at $V_{ds} = 5$ V and $V_{gs} = 0$ V, I_d collapse ratio (green crosses) defined as the after-stress pulsed I_d divided by after-stress quasi-static I_d at $V_{ds} = 5$ V and $V_{gs} = 0$ V, and the average pit depth as a function of stress time. The AlGaN/GaN HEMTs were stressed at (a) $V_{gs} = -7$ V and $V_{ds} = 43$ V in ambient air and (b) in a vacuum of 1×10^{-7} torr.

estimated by the formation rate of the surface pits using the following formula:

$$\mathrm{WVTR} \approx \frac{3}{2}\frac{V\rho M_{H_2O}}{MAt} \tag{10}$$

where $M_{H_2O} = 18$ g/mol is the molar mass of water and the rest of the symbols are the same as in (9). A calculation based on (10) shows that the minimum WVTR needed to cause the observed density and size of the pits is around 0.05–0.1 g/m^2/day, which matches well the typical value of the WVTR for PECVD SiN_y [28], [29].

With this rate, it takes only ~30 s to form a water layer at the interface between the SiN_y passivation and the III-N surface with a concentration of 1×10^{13} cm^{-2}. As the water reaches the III-N surface, reaction (1) occurs and the water molecules are consumed. For dry environment, the oxidation process will stop when all the water stored in the SiN_y passivation layer are consumed. This explains well why we could still observe a small amount of surface pits in vacuum [Fig. 2(b)] and in dry Ar [Fig. 4(b)]. On the other hand, for wet environment, the oxidation process will continuously occur due to the unlimited supply of water molecules from the atmosphere, and therefore the surface pits grow much larger [Figs. 2(a) and 4(a)].

VII. Relationship Between Structural and Electrical Degradation

Analyses on the drain current recorded in the experiment described in Section III have already showed that the drain current degradation was significantly suppressed in AlGaN/GaN HEMTs that were stressed in dry atmosphere (including vacuum) as compared to the HEMTs stressed in water-saturated atmosphere (including ambient air) for which the pits were large.

Here, we demonstrate the close relationship between drain current drop and the surface pits formation using time evolution measurements. Identical AlGaN/GaN HEMTs were stressed for different stress time from 1 ms to 10^4 s in air and in vacuum, respectively. It can be clearly seen in Fig. 12 that as the stress time increases, the drain current degradation (blue circles) follows the pit formation (red triangles) very well. The drain current collapse (green crosses) obtained by pulsed IV measurements with pulse width 250 ns also shows the same trend. It is therefore likely that the formation of the pits on the AlGaN surface impacts the drain current degradation [30]. One potential mechanism could be that the surface pits decreases the average thickness of the AlGaN barrier and thus decreases the average electron concentration in the channel, which leads to a higher access resistance and a lower drain current. It should be noted that as the oxidation is located at the gate edge and the area underneath the gate is not oxidized as shown in Fig. 3, the V_t largely remains unchanged.

On the other hand, as already shown in Fig. 1, the gate current degrades well before any pit formation and does not vary much with stress time. It seems that the I_g degradation might have a different origin altogether. This observation confirms some previous reports on the uncorrelated nature between gate current increase and output current drop [31]–[34]. One possible explanation, as suggested by Fig. 6, is that the migration of gallium might lead to trap states at the interface of gate metal and III-N layer, and thereby cause an increase in the gate leakage current. However, to fully understand this mass–transport process and its association with permanent gate current degradation, more work is needed in the future.

VIII. Conclusion

In conclusion, a mechanism involving water-assisted electrochemical reactions at the gate edge has been proposed to explain OFF-state structural degradation (surface pitting) in AlGaN/GaN HEMTs. We show that water from the passivation layer surface and the external atmosphere, as well as holes caused by trap-assisted interband tunneling in the AlGaN barrier are likely to play an essential role in forming the surface pits. Moreover, permanent drain current degradation has been explained by the reduction of the AlGaN barrier caused by surface pitting, while further investigation is still needed to fully understand the origin of the permanent gate current degradation.

References

[1] U. K. Mishra, P. Parikh, and Y.-F. Wu, "AlGaN/GaN HEMTs: An overview of device operations and applications," *Proc. IEEE*, vol. 90, no. 6, pp. 1022–1031, Jun. 2002.

[2] G. Meneghesso, G. Verzellesi, F. Danesin, F. Rampazzo, F. Zanon, A. Tazzoli, *et al.*, "Reliability of GaN high-electron-mobility transistors: State of the art and perspectives," *IEEE Trans. Device Mater. Rel.*, vol. 8, no. 2, pp. 332–343, Jun. 2008.

[3] J. A. del Alamo and J. Joh, "GaN HEMT reliability," *Microelectron Rel.*, vol. 49, no. 5, pp. 1200–1206, 2009.

[4] J. Joh and J. A. del Alamo, "Critical voltage for electrical degradation of GaN high-electron mobility transistors," *IEEE Electron Device Lett.*, vol. 29, no. 4, pp. 287–289, Apr. 2008.

[5] M. Meneghini, A. Stocco, M. Bertin, D. Marcon, A. Chini, G. Meneghesso, *et al.*, "Time-dependent degradation of AlGaN/GaN high electron mobility transistors under reverse bias," *Appl. Phys. Lett.*, vol. 100, no. 3, pp. 033505-1–033505-3, 2012.

[6] P. Marko, A. Alexewicz, O. Hilt, G. Meneghesso, E. Zanoni, J. Wurfl, *et al.*, "Random telegraph signal noise in gate current of unstressed and reverse-bias-stressed AlGaN/GaN high electron mobility transistors," *Appl. Phys. Lett.*, vol. 100, pp. 143507-1–143507-3, Feb. 2012.

[7] D. Marcon, T. Kauerauf, F. Medjdoub, J. Das, M. Van Hove, P. Srivastava, *et al.*, "A comprehensive reliability investigation of the voltage-, temperature- and device geometry-dependence of the gate dgradation on state-of-the-art GaN-on-Si HEMTs," in *Proc. IEEE IEDM*, Jan. 2010, pp. 1–20.

[8] A. Chini, M. Esposto, G. Meneghesso, and E. Zanoni, "Evaluation of GaN HEMT degradation by means of pulsed I-V, leakage and DLTS measurements," *IEEE Electron. Lett.*, vol. 45, no. 8, pp. 426–427, Apr. 2009.

[9] P. Makaram, J. Joh, J. A. del Alamo, T. Palacios, and C. V. Thompson, "Evolution of structural defects associated with electrical degradation in AlGaN/GaN high electron mobility transistors," *Appl. Phys. Lett.*, vol. 96, no. 23, pp. 233509-1–233509-3, 2010.

[10] F. Gao, B. Lu, L. Li, S. Kaun, J. S. Speck, C. V. Thompson, *et al.*, "Role of oxygen in the OFF-state degradation of AlGaN/GaN high electro mobility transistors," *Appl. Phys. Lett.*, vol. 99. no. 22, pp. 223506-1–223506-4, 2011.

[11] J. L. Jimenez, "GaN on SiC degradation modes and reliability evaluation," Tutorial given at ESREF, 2011.

[12] T. Hisaka, H. Sasaki, Y. Nogami, K. Hosogi, N. Yoshida, A. A. Villanueva, *et al.*, "Corrosion-induced degradation of GaAs PHEMTs under operation in high humidity conditions," *Microelectron. Rel.*, vol. 49, no. 12, pp. 1515–1519, 2009.

[13] A. Villanueva, J. A. del Alamo, T. Hisaka, and T. Ishida, "Drain corrosion in RF power GaAs PHEMTs," in *Proc. IEEE IEDM*, Dec. 2007, pp. 393–396.

[14] S. Nakahara and E. Kinsbron, "Room temperature interdiffusion study of Au/Ga thin film couples," *Thin Solid Films*, vol. 113, no. 1, pp. 15–26, Mar. 1984.

[15] D. Zhuang and J. H. Edgar, "Wet etching of GaN, AlN, and SiC: A review," *Mater. Sci. Eng., R, Rep.*, vol. 48, no. 1, pp. 1–46, 2005.

[16] C. Youtsey, I. Adesida, and G. Bulman, "Highly anisotropic photoenhanced wet etching of n-type GaN," *Appl. Phys. Lett.*, vol. 71, no. 15, pp. 2151–2153, 1997.

[17] M. S. Minsky, M. White, and E. L. Hu, "Room-temperature photoenhanced wet etching of GaN," *Appl. Phys. Lett.*, vol. 68, no. 11, pp. 1531–1533, 1996.

[18] K. Kunihiro, K. Kasahara, Y. Takahashi, and Y. Ohno, "Experimental evaluation of impact ionization coefficients in GaN," *IEEE Electron Device Lett.*, vol. 20, no. 12, pp. 608–610, Dec. 1999.

[19] B. Brar, K. Boutros, R. E. DeWames, V. Tilak, R. Shealy, and L. Eastman, "Impact ionization in high performance AlGaN/GaN HEMTs," in *Proc. IEEE Lester Eastman Conf. High Perform. Devices*, Aug. 2002, pp. 487–491.

[20] J. Kolnik, I. H. Oguzman, and F. Brennan, "Monte Carlo calculation of electron initiated impact ionization in bulk zinc-blende and wurtzite GaN," *J. Appl. Phys.*, vol. 81, no. 2, pp. 726–733, 1999.

[21] C. Bulutay, "Electron initiated impact ionization in AlGaN alloys," *Semicond. Sci. Technol.*, vol. 17, no. 10, pp. L59–L62, 2002.

[22] L. V. Keldysh, "Behavior of non-metallic crystals in strong electric field," *Soviet Phys. JETP*, vol. 33, no. 4, pp. 763–770, 1958.

[23] E. O. Kane, "Theory of tunneling," *J. Appl. Phys.*, vol. 32, no. 1, pp. 83–89, 1961.

[24] G. A. M. Hurkx, D. B. M. Klaassen, and M. P. G. Knuvers, "A new recombination model for device simulation including tunneling," *IEEE Trans. Electron Devices*, vol. 39, no. 2, pp. 331–338, Mar. 1992.

[25] V. Bougrov, M. E. Levinshtein, S. L. Rumyantsev, and A. Zubrilov, *Properties of Advanced Semiconductor Materials GaN, AlN, InN, BN, SiC, SiGe*, M. E. Levinshtein, S. L. Rumyantsev, and M. S. Shur, Eds. New York, NY, USA: Wiley, 2001, pp. 1–30.

[26] E. J. Miller, X. Z. Dang, and E. T. Yu, "Gate leakage current mechanisms in AlGaN/GaN heterostructure field-effect transistors," *J. Appl. Phys.*, vol. 88, no. 10, pp. 5851–5958, 2000.

[27] M. A. Henderson, "The interaction of water with solid surfaces: Fundamental aspects revisited," *Surf. Sci. Rep.*, vol. 46, nos. 1–8, pp. 1–308, 2002.

[28] A. S. da Silva Sobrinho, M. Latreche, G. Czeremuszkin, J. E. Klemberg-Sapieha, and M. R. Wertheimer, "Transparent barrier coatings on polyethylene terephthalate by single- and dual-frequency plasma-enhanced chemical vapor deposition," *J. Vac. Sci. Technol. A*, vol. 16, no. 6, pp. 3190–3198, 1998.

[29] D. S. Wuu, W. C. Lo, C. C. Chiang, H. B. Lin, L. S. Chang, R. H. Horng, *et al.*, "Water and oxygen permeation of silicon nitride films prepared by plasma-enhanced chemical vapor deposition," *Surf. Coat. Technol.*, vol. 198, nos. 1–3, pp. 114–117, 2004.

[30] J. Joh, J. A. del Alamo, K. Langworthy, S. Xie, and T. Zheleva, "Correlation between electrical and material degradation in GaN HEMTs stressed beyond the critical voltage," *Microelectron. Rel.*, vol. 51, no. 2, pp. 201–206, 2011.

[31] D. Marcon, J. Viaene, P. Favia, H. Bender, X. Kang, S. Lenci, *et al.*, "Reliability of AlGaN/GaN HEMTs: Permanent leakage current increase and output current drop," *Microelectron. Rel.*, vol. 52, nos. 9–10, pp. 2188–2193, 2012.

[32] B. D. Christiansen, R. A. Coutu, E. R. Heller, B. S. Poling, G. D. Via, R. Vetury, *et al.*, "Reliability testing of AlGaN/GaN HEMTs under multiple stressors," in *Proc. IEEE IRPS*, Apr. 2011, pp. CD.2.1–CD.2.5.

[33] J. L. Jimenez and U. Chowdhury, "X-band GaN FET reliability," in *Proc. IEEE IRPS*, May 2008, pp. 429–435.

[34] J. Joh and J. A. del Alamo, "Time evolution of electrical degradation under high-voltage stress in GaN high electron mobility transistors," in *Proc. IEEE IRPS*, Apr. 2011, pp. 4E.3.1–4E.3.4.

Feng Gao received the B.S. degree in physics from Fudan University, Shanghai, China, in 2008. He is currently pursuing the Ph.D. degree in materials science and engineering with the Massachusetts Institute of Technology, Cambridge, MA, USA.

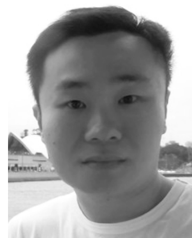

Swee Ching Tan received the bachelor's degree in physics from the National University of Singapore, Singapore, and the Ph.D. degree from the Electrical Engineering Department, University of Cambridge, Cambridge, U.K.

He is currently a Post-Doctoral Associate with the Department of Material Science and Engineering, Massachusetts Institute of Technology, Cambridge, MA, USA.

Jesús A. del Alamo (S'79–M'85–SM'92–F'06) received the Ph.D. degree in electrical engineering from Stanford University, Stanford, CA, USA, in 1985.

He is currently a Donner Professor and MacVicar Faculty Fellow with the Massachusetts Institute of Technology, Cambridge, MA, USA.

Carl V. Thompson received the S.B. degree in materials science and engineering from the Massachusetts Institute of Technology (MIT), Cambridge, MA, USA, in 1976, and the Ph.D. degree in applied physics from Harvard University, Cambridge, in 1982.

He is the Stavros Salapatas Professor of materials science and engineering and the Director of the Materials Processing Center, MIT.

Tomás Palacios (M'97–SM'13) is the Emmanuel Landsman CD Associate Professor with the Department of Electrical Engineering and Computer Science, Massachusetts Institute of Technology, Cambridge, MA, USA. His current research interests include the combination of new semiconductor materials and device concepts to advance the fields of information technology, biosensors, and energy conversion.